


Quantitative choriocapillaris evaluation in intermediate age-related macular degeneration by swept-source optical coherence tomography angiography

Stela Vujosevic,¹  Caterina Toma,¹ Edoardo Villani,^{2,3} Andrea Muraca,¹ Emanuele Torti,⁴ Giordana Florimbi,⁴ Marco Pezzotti,¹ Paolo Nucci^{2,3} and Stefano De Cilla^{1,5}

¹Eye Clinic, University Hospital Maggiore della Carita', Novara, Italy

²Department of Clinical Sciences and Community Health, University of Milan, Milan, Italy

³Eye Clinic San Giuseppe Hospital, Milan, Italy

⁴Department of Electrical, Computer and Biomedical Engineering, University of Pavia, Pavia, Italy

⁵Department of Health Sciences, University East Piedmont "A.Avogadro", Novara, Italy

ABSTRACT.

Purpose: To investigate choriocapillaris (CC) perfusion, by evaluating flow voids (FV), in eyes with intermediate age-related macular degeneration (iAMD) using swept-source optical coherence tomography angiography (SS-OCT-A).

Methods: Patients with bilateral or unilateral iAMD and normal controls underwent SS-OCT and OCT-A examination. Choriocapillaris (CC) FVs were quantitatively assessed on OCT-A images using MATLAB (version 2017b; MathWorks, Natick, MA, USA), after a preprocessing aimed at compensating for CC attenuation artefacts. Three different thresholds [1 standard deviation (SD), 1.25 SD and 1.5 SD] were applied. Final FV percentage (FV%) was calculated as the ratio between area with absent flow and total scanned area.

Results: Of 41 patients with iAMD and 16 normal subjects enrolled in the study, 39 eyes (39 patients) with iAMD and all 16 normal eyes (16 control subjects) were included in the final analysis. Mean FV% (1 SD) was 13.45 ± 0.66 in controls, 14.19 ± 1.23 in bilateral iAMD and 14.21 ± 0.99 in unilateral iAMD ($p = 0.03$, for difference between controls and bilateral iAMD). Mean FV% (1.25 SD) was 6.55 ± 0.65 in controls, 7.33 ± 1.4 in bilateral iAMD and 7.06 ± 1.4 in unilateral iAMD ($p = 0.048$, for difference between controls and bilateral iAMD). Mean FV% (1.5 SD) was 2.71 ± 0.82 in controls, 2.55 ± 1.12 in bilateral iAMD and 3.25 ± 1.17 in unilateral iAMD ($p = 0.038$, for difference between bilateral and unilateral iAMD).

Conclusion: A significantly higher FV% was found in patients with iAMD versus controls. A higher trend in FV% was found in unilateral iAMD (with neovascular AMD in the fellow eye) versus bilateral iAMD, when applying the lowest threshold. Further, larger and longitudinal studies are needed to confirm this data.

Key words: artefacts – choriocapillaris – drusen – flow voids – intermediate age-related macular degeneration – swept-source OCT angiography

Introduction

Age-related macular degeneration (AMD) is one of the leading causes of visual impairment in the elderly worldwide, with an estimated global prevalence of 196 million affected individuals and an estimated rise of approximately 40% by 2040 (Wong et al. 2014; Seddon 2017). Several classification systems have been proposed over time to define the natural course of AMD. The most used in the past was the four-stage classification by the Age-Related Eye Disease Study group, dividing AMD into an early (stage 1 and 2), intermediate (stage 3) and late (stage 4) disease (Age-related Eye Disease Study Research Group 2000). In 2013, a new five-stage clinical classification of AMD was proposed by the Beckman Initiative for Macular Research Classification Committee in order to better define the risk of progression to the late stages of disease (Ferris et al. 2013). Stage 1 corresponds to absence of disease, stage 2 to normal ageing fundus changes, defined as the presence of only small drusen (dimension $< 63 \mu\text{m}$) without retinal pigment epithelium (RPE) changes, stage 3 to early disease characterized by medium-size drusen ($> 63 \mu\text{m}$; $\leq 125 \mu\text{m}$) without RPE changes, stage 4 to intermediate AMD with large drusen ($> 125 \mu\text{m}$)

Acta Ophthalmol. 2019; 97: e919–e926

© 2019 Acta Ophthalmologica Scandinavica Foundation. Published by John Wiley & Sons Ltd

doi: 10.1111/aos.14088

and/or RPE changes, stage 5 to late AMD due to presence of choroidal neovascularization or geographic atrophy (GA) (Ferris et al. 2013). Both of these classification systems are based on fundus photography and do not take into account information derived from other non-invasive or invasive imaging techniques, such as optical coherence tomography (OCT), autofluorescence, OCT angiography (OCT-A), fluorescein or indocyanine green angiography (FFA, ICGA) (Miller et al. 2017).

In patients with drusen, standard imaging techniques (OCT and dye-based angiography) proved to be particularly useful in detecting and defining the presence of choroidal neovascularization [neovascular AMD (nAMD)], but with intrinsic limits in detailed visualization of choriocapillaris (CC) and choroid (Bischoff & Flower 1985; Flower 1993; Zhu et al. 2006). Recently, a new diagnostic method, OCT-A, has been introduced into clinical practice for a non-invasive evaluation of patients affected by AMD. On OCT-A scans, CC can be visualized as an alternation of dark areas (called signal voids), where CC flow is undetectable, and granular bright areas that are indicative of preserved flow (Spaide et al. 2015; Spaide 2016, 2017). Signal voids may represent areas of real CC nonperfusion (flow voids) or, alternatively, areas where flow signal strength is below the decorrelation threshold (Choi et al. 2015; Spaide et al. 2015; Spaide 2017). Optical coherence tomography angiography (OCT-A) in eyes with drusen shows different patterns and severity of CC flow impairment depending on drusen extent and location (Chatziralli et al. 2018). In advanced stages of AMD such as GA, OCT-A showed CC impairment both underlying the area of GA (with displacement of larger choroidal vessels at CC level) (Waheed et al. 2016) and extending beyond its borders, even with RPE preservation (Choi et al. 2015; Kvanta et al. 2017). In nAMD, OCT-A could be helpful in detecting and better defining neovascular membranes choroidal neovascularization (CNV) (Carnevali et al. 2016; de Oliveira Dias et al. 2018). However, it is important to pay attention to frequent presence of attenuation artefacts (for example due to presence of drusen) and projection

artefacts from superficial vessels, when evaluating CC images obtained with OCT-A (Cole et al. 2017; Spaide et al. 2018). Swept-source (SS) OCT-A devices use a longer wavelength (1050 nm); thus, they have a better ability to penetrate deeper into tissues beneath the RPE, making these instruments more reliable in the evaluation of CC than spectral domain devices, that use a shorter wavelength (McLeod et al. 2002; Bloom & Singal 2011; Pepple & Mruthyunjaya 2011; Choi et al. 2013; Lane et al. 2016; Alten et al. 2017).

The purpose of this study is to analyse CC of eyes affected by intermediate AMD (iAMD) using SS-OCT-A, by performing quantitative measurement of CC flow voids (FVs; after removing artefacts), in order to investigate if any reduction in flow signal is present at this level.

Materials and Methods

Study participants

In this prospective cross-sectional comparative study, we consecutively enrolled 41 eyes of 41 patients affected by unilateral or bilateral iAMD, who presented at Medical Retina Service, University Hospital Maggiore della Carità, Novara, Italy, between July 2017 and September 2018. Diagnosis of iAMD was based on detection of large soft drusen with or without RPE pigmentary changes on fundus examination and confirmed with OCT (Ferris et al. 2013). In addition, 16 normal eyes of 16 age-matched subjects were enrolled as the control group. For patients with bilateral iAMD and healthy controls, the right eye was included in the study, except when poor quality of OCT-A images precluded a reliable analysis.

Inclusion criteria for the study were as follows: diagnosis of iAMD in one or both eyes and good quality OCT and OCT-A images. Exclusion criteria were as follows: presence of systemic pathologies that could affect retinal and choroidal microcirculation, in particular diabetes mellitus type 1 and 2 and uncontrolled systemic blood pressure ($\geq 120/80$ mmHg) (Mancia et al. 2013); presence of exudative changes suggestive of nAMD or presence of GA on fundus examination and OCT (Fleckenstein et al. 2008); any maculopathy other than AMD

(e.g. diabetic or tractional maculopathy); previous vitreoretinal surgery or use of anti-vascular endothelial growth factor (VEGF) drugs; use of any drug known to interfere with macular function (e.g. hydroxychloroquine, tamoxifen); refractive error $>\pm 4$ D; poor quality OCT and/or OCT-A images. Normal controls were recruited among healthy subjects with no significant media opacity and normal fundus examination that underwent a routine annual eye examination.

Each patient underwent a complete eye examination including dilated fundus examination with 90 D lens, SS-OCT and SS-OCT-A. Patients with features suspect for the presence of CNV on OCT-A, despite the complete absence of exudative changes on fundus examination and OCT, were further investigated with FFA and ICGA in order to confirm or exclude the diagnosis of subclinical CNV. Eyes with CNV confirmed on FFA and/or ICGA were excluded from the final analysis.

The study adhered to the tenets of the Declaration of Helsinki and was approved by the Ethics Committee; signed informed consent was obtained from all patients.

Imaging

Optical coherence tomography (OCT) and OCT-A images were taken using DRI SS-OCT Triton plus (Topcon Medical Systems Europe, Milano, Italy). The device uses a wavelength of 1050-nm, with a speed of acquisition of 100 000 A-scans/second. It is equipped with an active eye tracker for reducing motion artefacts. This OCT-A instrument preserves axial resolution using an innovative motion contrast measure named OCT-A ratio analysis.

A trained operator performed the following scans: an OCT three-dimensional (3D) macula map covering an area of 7 mm \times 7 mm, a 9 mm radial OCT scan (consisting of 12 scans 15° apart) centred on the fovea, a single 6-mm high-definition B-scan at 0° and 90° and a 3D 4.5 \times 4.5 mm OCT-A map of the macula.

All OCT-A images were carefully reviewed to check automated segmentation of CC. The CC slab was obtained from Bruch's membrane (BM) to 10.4 μ m below BM. In case

of errors, manual correction was performed.

In case of suspect CNV, FFA and ICGA were performed with Spectralis HRA-OCT (confocal scanning laser ophthalmoscope and angiography; HRA2, Heidelberg Engineering, Heidelberg, Germany).

Image analysis

Two trained graders (C.T. and A.M.) evaluated all OCT and OCT-A images, and in case of disagreement the final adjudication was given by the experienced retinal specialist (S.V.). All images were saved and analysed in anonymous and masked fashion.

Optical coherence tomography (OCT) scans were used to confirm the diagnosis of iAMD based on the presence of drusen and RPE pigmentary changes. In addition, OCT B-scans were carefully evaluated to detect any sign of exudative changes, such as intraretinal and/or subretinal fluid (intraretinal cysts, serous or haemorrhagic

detachment of the neuroretina), and presence of RPE detachment. Choroidal thickness (CT) was evaluated using the automatic segmentation of 3D macula map obtained with DRI OCT Triton plus instrument (software version 10.07.003.03). The instrument automatically calculated CT in 9 Early Treatment Diabetic Retinopathy study (ETDRS) areas. Only the central sub-field CT (within 1 central millimetre diameter, centred on the fovea) was considered for the analysis.

Choriocapillaris (CC) OCT-A slabs were first qualitatively evaluated to exclude the presence of CNV (Fig. 1) and then used for quantitative assessment of CC, using the automatic segmentation algorithm present in the device. Quantitative measurement consisted of evaluation of CC flow voids, performed using image processing function of MATLAB (version 2017b, MathWorks, Natick, MA, USA). Images of poor quality due to artefacts (e.g. motion artefacts) and low-quality signal (<50) were excluded from the analysis.

In order to calculate CC flow voids, a recently published and validated method to compensate for CC attenuation artefacts due to drusen was applied (Zhang et al. 2018). In summary, OCT-A flow images and corresponding en face CC structural images were exported from the OCT-A device and imported into MATLAB. An inverse transformation and a Gaussian smoothing filter were applied to structural image to enhance the signal under drusen and minimize speckle noise. Then, a multiplication between the flow image (F_{CC}) and the transformed structural image ($1 - \text{Norm}(S_{CC})$) was performed:

$$F_{\text{compensated}} = F_{CC} \times (1 - \text{Norm}(S_{CC})).$$

Finally, the compensated CC flow image was obtained. In addition, projections artefacts due to superficial retinal vessels were eliminated using a previously published method (Borrelli

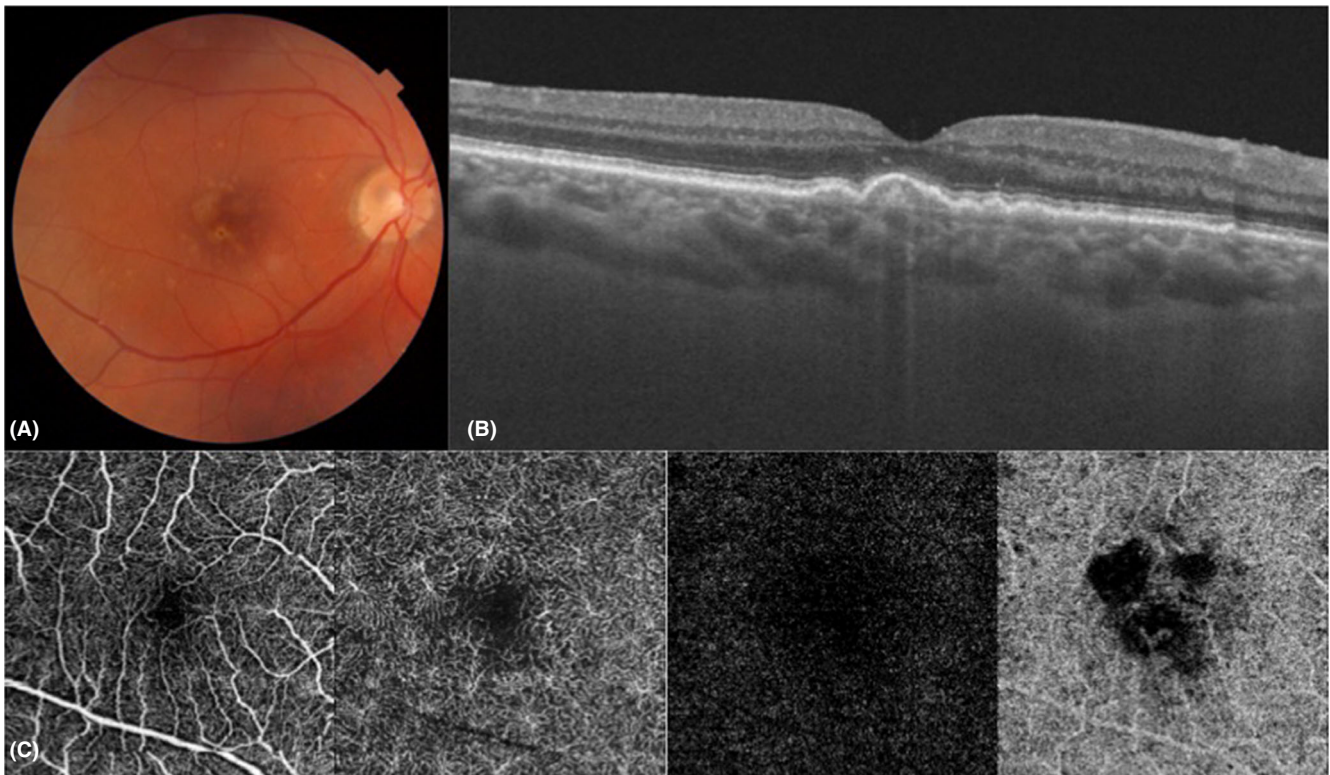


Fig. 1. Right eye of a patient with bilateral intermediate AMD. (A) Colour fundus photography showing confluent large soft drusen associated with RPE pigmentary changes. (B) Structural OCT horizontal scan centred on the fovea showing multiple drusen, with no signs of exudation (intraretinal and/or subretinal fluid). (C) Optical coherence tomography angiography (OCT-A) slabs automatically segmented at the SCP, DCP, outer retina and CC level (from left to right): SCP, DCP and outer retina show no significant alterations; CC image shows multiple areas of reduced or absent signal, due to both presence of attenuation artifacts and real reduced blood flow. No signs of neovascularization are visible on OCT-A. AMD = age-related macular degeneration, CC = choriocapillaris, DCP = deep capillary plexus, OCT = optical coherence tomography, OCT-A = OCT-angiography, RPE = retinal pigment epithelium, SCP = superficial capillary plexus.

et al. 2017b). Main image processing steps are reported in Fig. 2.

Flow voids (FVs) were calculated as a percentage between area with absence of flow ($Area_{Flowvoid}$) and total scanned area ($Area_{whole}$):

$$FV = \frac{Area_{Flowvoid}}{Area_{whole}} \times 100\%$$

$Area_{Flowvoid}$ was determined using three different levels of thresholding, [1 standard deviation (SD), 1.25 SD and 1.5 SD], as previously proposed (Zhang et al. 2018).

Statistical analysis

Age was compared among the three subject groups using one-way ANOVA. Analysis of covariance (ANCOVA) was employed to compare clinical variables [CT and flow voids percent (FV%)] among the three subject groups (controls, bilateral iAMD, unilateral iAMD) by adjusting for age (Pocock et al. 2002). The means of populations were estimated as least squares means, which are the best linear estimates for the marginal means in the ANCOVA design. In case of an overall statistically significant difference among subject groups, pairwise comparisons among the three

groups were done using the Scheffé test (Howell 2010). All the analyses were performed using STATISTICAL VERSION software 6.0 (StatSoft Inc., Tulsa, OK, USA), using a two-sided type I error rate of $p = 0.05$.

Results

Study population characteristics

Of the initially enrolled 41 eyes with diagnosis of iAMD, two eyes were excluded for detection of suspect sub-clinical CNV on OCT-A and confirmed on FFA/ICGA. Therefore, 39 eyes of 39 patients (24 females and 15 males) and 16 normal eyes of 16 controls were included in the final analysis. Of 39 eyes with iAMD, 26 eyes (66.7%) had bilateral iAMD, while 13 (33.3%) had iAMD in one eye and nAMD (presence of CNV) in the fellow eye. Mean age was 72.4 ± 8.02 years (range: 60–89) in healthy controls and 75.7 ± 7.89 years (range: 56–89) in the entire iAMD population, 74.8 ± 7.53 years (range: 59–87) in the bilateral iAMD group and 77.69 ± 8.57 (range: 56–89) in the group with nAMD in the fellow eye. Age was not significantly different among the three study groups ($p = 0.21$).

OCT data

Mean CT was $258 \pm 89.91 \mu m$ in controls, $181 \pm 66.46 \mu m$ in patients with bilateral iAMD and $174 \pm 84.26 \mu m$ in patients with unilateral iAMD. A statistically significant difference was found between controls and unilateral iAMD ($p = 0.03$). There was no significant difference between controls and bilateral iAMD ($p = 0.06$) and between unilateral and bilateral iAMD ($p = 0.58$).

OCT-A data

All row data of the included patients and subjects are shown in Table 1. Mean FV% (1 SD) was 13.45 ± 0.66 in controls, 14.19 ± 1.23 in patients with bilateral iAMD and 14.21 ± 0.99 in patients with nAMD in the fellow eye. An increasing trend from controls to bilateral iAMD and to unilateral iAMD was found, with a statistically significant difference between controls and bilateral iAMD ($p = 0.03$) and a border-line statistically significant difference between controls and unilateral iAMD ($p = 0.05$). Mean FV% (1.25 SD) was 6.55 ± 0.65 in controls, 7.33 in patients with bilateral iAMD and 7.06 ± 1.4 in patients with unilateral iAMD. A statistically significant

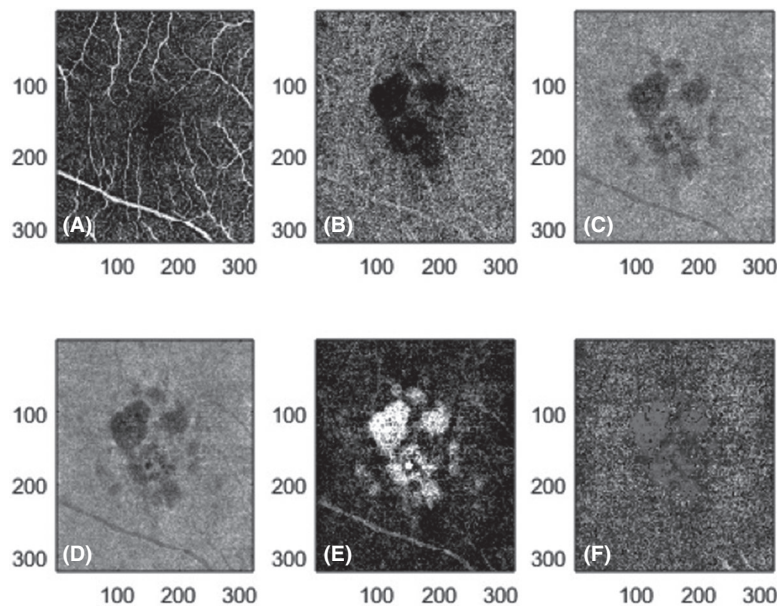


Fig. 2. Image processing steps performed to compensate for CC attenuation artifacts due to the presence of drusen. (A) Original SCP optical coherence tomography angiography (OCT-A) image; (B) original CC OCT-A image; (C) original en face structural CC image; (D) en face structural CC image after Gaussian smoothing filter application; (E) en face structural CC image after inverse transformation ($1 - Norm(C)$, transformed structural CC image); (F) projection artefact-free and compensated CC flow image obtained from the multiplication between the flow image (B) and the transformed structural image (E). CC = choriocapillaris, SCP = superficial capillary plexus.

Table 1. Choriocapillaris flow voids percentage of each subject/patient included in the final analysis of the study.

Normal controls	FV% (1 SD)	FV% (1.25 SD)	FV% (1.5 SD)	Bilateral iAMD	FV% (1 SD)	FV% (1.25 SD)	FV% (1.5 SD)	Unilateral iAMD	FV% (1 SD)	FV% (1.25 SD)	FV% (1.5 SD)
1	13.68	6.63	2.35	1	14.58	7.21	2.09	1	13.48	8.10	4.67
2	14.82	7.43	2.26	2	14.21	7.22	1.53	2	15.24	8.64	4.54
3	13.70	7.11	3.87	3	13.41	6.96	2.05	3	13.88	7.70	3.89
4	13.96	6.39	1.94	4	15.07	7.17	1.61	4	14.18	7.41	3.68
5	13.87	7.55	3.39	5	13.63	6.21	2.97	5	14.82	7.26	3.47
6	14.05	6.40	2.23	6	14.6	10.31	2.24	6	12.84	6.70	3.70
7	12.88	5.57	2.10	7	17.68	4.25	3.14	7	15.05	7.50	1.36
8	13.68	6.58	2.26	8	13.78	7.73	2.75	8	13.07	6.22	1.65
9	13.37	6.22	1.90	9	15.7	9.13	4.65	9	16.04	3.12	2.29
10	12.60	6.03	2.05	10	14.09	7.37	1.94	10	13.59	7.18	3.89
11	13.22	6.22	3.29	11	13.60	7.33	1.71	11	13.68	6.16	1.32
12	13.34	6.41	2.41	12	14.14	7.24	1.21	12	15.38	8.46	3.99
13	13.39	6.46	2.30	13	14.57	8.06	1.85	13	13.53	7.27	3.82
14	12.16	5.54	2.81	14	13.17	7.18	3.98				
15	12.61	6.37	3.50	15	12.80	6.32	2.82				
16	13.84	7.88	4.77	16	15.33	8.02	2.24				
				17	14.32	9.21	2.92				
				18	15.52	8.04	1.69				
				19	14.40	7.64	1.89				
				20	13.67	9.32	6.02				
				21	13.97	6.94	1.48				
				22	11.27	5.66	2.91				
				23	13.52	8.35	2.13				
				24	13.15	6.51	1.39				
				25	15.91	3.97	3.00				
				26	13.01	7.47	4.01				

FV = flow void, iAMD = intermediate age-related macular degeneration, SD = standard deviation.

Table 2. Mean choriocapillaris flow voids percentage of study groups evaluated on swept-source OCT angiography.

Group	FV% (1 SD)	FV% (1.25 SD)	FV% (1.5 SD)
Controls (<i>n</i> = 16)	13.45 ± 0.66	6.55 ± 0.65	2.71 ± 0.82
Bilateral iAMD (<i>n</i> = 26)	14.19 ± 1.23*	7.33 ± 1.4 [†]	2.55 ± 1.12
Unilateral iAMD (<i>n</i> = 13)	14.21 ± 0.99	7.06 ± 1.4	3.25 ± 1.17 [‡]

One-way analysis of covariance analyses by adjusting for age: comparison among controls, patients with bilateral iAMD and patients with unilateral iAMD. One eye per patient/subject was evaluated. Statistical significance was set at *p* = 0.05. FV% is reported as mean ± SD.

FV = flow void, iAMD = intermediate age-related macular degeneration, *n* = number of patients, SD = standard deviation.

Comparison versus controls: *Scheffè test, *p* = 0.03, [†]Scheffè test, *p* = 0.048.

Comparison versus bilateral iAMD: [‡]Scheffè test, *p* = 0.038.

difference was found between controls and bilateral iAMD (*p* = 0.048), and no statistically significant difference was found between controls and unilateral iAMD (*p* = 0.28). Mean FV% (1.5 SD) was 2.71 ± 0.82 in controls, 2.55 ± 1.12 in patients with bilateral iAMD and 3.25 ± 1.17 in patients with unilateral iAMD. A statistically significant difference was found between bilateral and unilateral iAMD, *p* = 0.038, and no statistically significant difference was found between controls and unilateral iAMD (*p* = 0.15). Flow voids percent (FV%)

results (mean ± SD) with different methods of thresholding are summarized in Table 2.

Discussion

In this study, we prospectively investigated CC alterations in patients with iAMD by means of SS-OCT-A. Quantitative evaluation of FVs was used as a measure of CC impairment, documenting a significant reduction in CC blood flow in eyes with iAMD compared to healthy controls.

Previous studies, performed using laser Doppler flowmetry, have demonstrated a progressive decline in density and diameter of CC and medium-sized choroidal vessels with age, that seems to be faster and more accentuated in patients with AMD (Grunwald et al. 1998a,b, 2005; Metelitsina et al. 2008). Enhanced depth imaging spectral domain m(SD)-OCT has shown a decrease in CT over decades (Spaide et al. 2008; Margolis & Spaide 2009; Ding et al. 2011). Histologic studies have demonstrated the presence of regions of CC impairment in relation to drusen formation even in the earliest stages of AMD, with lower choroidal vascular density in patients with higher number of drusen and sub-RPE deposits (Mullins et al. 2011). Post-mortem analyses on choroids from human donors have tried to clarify the connection between RPE and CC loss in AMD. In nAMD, areas of CC dropout were observed surrounding both active and inactive CNV, even when RPE was preserved (McLeod et al. 2009). As proposed by Bhutto and Lutty, this may indicate that in nAMD the first damage could be at the CC level, as a result of an ischaemic and/or

inflammatory insult (Bhutto & Luty 2012), with consequent disruption of RPE/Bruch's complex and loss of photoreceptors (Zarbin & Rosenfeld 2010; Querques et al. 2014; Borrelli et al. 2017a). Instead, in GA the initial insult seems to be at the level of RPE, whereas dysfunction and death of photoreceptors and CC appear to be a secondary event (Bhutto & Luty 2012).

Swept-source (SS)-OCT-A has introduced new insights into the evaluation of CC in AMD. Even if CC flow quantification is still challenging, different approaches have been tried in previous studies. These include signal binarization, analysis of decorrelation signal indices and of signal voids and vascular and perfusion density measurement (Alten et al. 2016; Spaide 2016, 2017; Cicinelli et al. 2017; Nicolò et al. 2017; Lauermann et al. 2018). Nesper et al. (2017) proposed an algorithm to calculate CC nonperfused area in patients with reticular pseudodrusen (RPD) and drusen, excluding areas of CC underlying drusen and superficial retinal vessels, as potential sources of artefacts. Lane et al. (2016) performed a study comparing SS and SD-OCT-A devices in early and intermediate AMD, concluding that SS technology produced fewer areas of false-positive flow impairment (thus being capable of better discriminating between all signal voids and real flow voids). In the present study, we performed SS-OCT-A in eyes with diagnosis of iAMD in order to better define CC changes that occur in this disease. Choriocapillaris (CC) changes were evaluated by quantifying FVs, after compensating for attenuation artefacts and removal of projection artefacts.

The percentage of FVs was compared among patients with bilateral and unilateral iAMD and healthy controls. Patients with unilateral iAMD had nAMD in the fellow eye. We found a significantly higher percentage of FVs in pathologic eyes versus normal eyes, with slightly higher values detected in unilateral iAMD eyes versus bilateral iAMD eyes when applying the lowest threshold (1 SD) and significantly higher values when applying the highest threshold. The issue of the optimal threshold value to be used in CC analysis still remains open. In agreement with the study by Zhang et al. (2018), larger thresholds resulted in

fewer FVs and viceversa. However, if the threshold is too high, only few pixels are accounted as $Area_{Flowvoid}$; therefore, it is possible that some FVs are missed and that the whole $Area_{Flowvoid}$ is not entirely considered. On the other hand, if the threshold is too low, a certain amount of pixels could be erroneously taken into account during FVs computation, increasing the number of false positives in the considered area. In the present study, three different threshold values were tested and the 1 SD threshold showed the most significant difference in measuring FVs both in normal controls and iAMD cases. However, it is important to highlight that there is no gold standard for results validation; thus, the accuracy of the proposed method was based on a visual evaluation of final compensated images, as recently proposed (Zhang et al. 2018). In the present study, the 1 SD threshold was capable of well distinguishing healthy controls from pathologic eyes and a slight difference, even if not statistically significant, was found also between unilateral and bilateral iAMD cases. If we consider the 1.25 threshold, it was still possible to discriminate between healthy and pathological cases, but the possibility to differentiate unilateral from bilateral iAMD cases was lost. Considering the 1.5 SD threshold, it was only possible to distinguish unilateral from bilateral iAMD cases, but without the possibility to correctly identify healthy controls.

Our results are in agreement with a recent study by Borrelli et al. (2017a,b) that, with a different method of analysis, detected a higher average CC signal void size in patients with iAMD in one eye and nAMD in the fellow eye. Moreover, a higher average CC signal void size was reported in eyes with early and iAMD and type 3 neovascularization in the fellow eye versus early and iAMD and type 1 or 2 neovascularization in the fellow eye (Borrelli et al. 2018a,b,c). It is clearly established that patients with nAMD in one eye have a higher risk of developing nAMD in the fellow eye, therefore, these data may support the hypothesis that CC impairment could drive the development of neovascular form of AMD. Other recent studies evaluated CC in the early stages of AMD using OCT-A. Cicinelli et al. (2017) used OCT-A to evaluate CC vascular

density on binarized images in patients with drusen and RPD reporting decreased density in comparison with healthy controls. Chatziralli et al. (2018) performed OCT-A in patients with early AMD and qualitatively described a reduction in CC blood flow signal that in some patients extended beyond the drusen area (although without excluding potential source of artefacts from the image evaluation). Borrelli et al. (2018a) used SS-OCT-A to evaluate eyes with iAMD and found a significant CC flow impairment (increased signal void area compared to healthy controls) that topographically corresponded to the area covered by drusen.

Although iAMD is often characterized by preserved visual acuity (Friedman et al. 2004), CC is essential for maintaining a proper photoreceptor function. Thus, the reduction in CC flow, described in patients with iAMD, may affect photoreceptor structure and function (Borrelli et al. 2018b), leading to impaired macular function. Nesper et al. (2017) found that nonperfused CC area detected on OCT-A correlated to decreased visual acuity in a group of eyes with drusen and pseudodrusen; Borrelli et al. (2018c) observed a correlation between FVs area and N1 multifocal electroretinogram implicit times in iAMD, thus supporting the hypothesis of an association between CC perfusion and photoreceptor function.

The major limitations of the present study include a small sample size and a lack of a longitudinal follow-up. However, the use of both swept-source technology and the process of compensation of attenuation artefacts in image analyses, allowed to significantly improve the reliability of the results, thus making it the major strengths of this study.

At the best of our knowledge, even if small in numbers, this is the first study to apply this novel method of CC perfusion analysis to compare bilateral and unilateral cases of iAMD. Higher values of FV% were detected in patients with iAMD versus normal controls and an increasing trend was found from patients with bilateral iAMD to patients with nAMD in the fellow eye. If these observations could be confirmed in future larger longitudinal studies, this may be an element in support of the hypothesis of CC impairment as a

possible primum movens of the neovascular form of AMD that can be clinically detected and evaluated with a non-invasive method.

In conclusion, the present study documents a reduction in CC blood flow in patients affected by iAMD. Optical coherence tomography angiography (OCT-A) should be considered an important non-invasive imaging modality for the study of patients with iAMD. Further longitudinal studies including larger sample of patients are necessary to confirm these preliminary data and to investigate the rate and timing of development of nAMD in patients with reduced CC blood flow.

References

- Age-Related Eye Disease Study Research Group (2000): Risk factors associated with age-related macular degeneration: a case-control study in the age-related eye disease study: age-related eye disease study report number 3. *Ophthalmology* **107**: 2224–2232.
- Alten F, Heiduschka P, Clemens CR & Eter N (2016): Exploring choriocapillaris under reticular pseudodrusen using OCT-angiography. *Graefes Arch Clin Exp Ophthalmol* **254**: 2165–2173.
- Alten F, Laueremann JL, Clemens CR, Heiduschka P & Eter N (2017): Signal reduction in choriocapillaris and segmentation errors in spectral domain OCT angiography caused by soft drusen. *Graefes Arch Clin Exp Ophthalmol* **255**: 2347–2355.
- Bhutto I & Luty G (2012): Understanding age-related macular degeneration (AMD): relationships between the photoreceptor/retinal pigment epithelium/Bruch's membrane/choriocapillaris complex. *Mol Aspects Med* **33**: 295–317.
- Bischoff PM & Flower RW (1985): Ten years experience with choroidal angiography using indocyanine green dye: a new routine examination or an epilogue? *Doc Ophthalmol* **60**: 235–291.
- Bloom SM & Singal IP (2011): The outer Bruch membrane layer: a previously undescribed spectral-domain optical coherence tomography finding. *Retina* **31**: 316–323.
- Borrelli E, Abdelfattah NS, Uji A, Nittala MG, Boyer DS & Sadda SR (2017a): Postreceptor neuronal loss in intermediate age-related macular degeneration. *Am J Ophthalmol* **181**: 1–11.
- Borrelli E, Uji A, Sarraf D & Sadda SR (2017b): Alterations in the choriocapillaris in intermediate age-related macular degeneration. *Invest Ophthalmol Vis Sci* **58**: 4792–4798.
- Borrelli E, Mastropasqua R, Senatore A, Palmieri M, Toto L, Sadda SV & Mastropasqua L (2018a): Impact of choriocapillaris flow on multifocal electroretinography in intermediate age-related macular degeneration eyes. *Invest Ophthalmol Vis Sci* **59**: AMD25–AMD30.
- Borrelli E, Shi Y, Uji A, Balasubramanian S, Nassisi M, Sarraf D & Sadda SR (2018b): Topographical analysis of the choriocapillaris in intermediate age-related macular degeneration. *Am J Ophthalmol* **196**: 34–43.
- Borrelli E, Souied EH, Freund KB et al. (2018c): Reduced choriocapillaris flow in eyes with type 3 neovascularization and age-related macular degeneration. *Retina* **38**: 1968–1976.
- Carnevali A, Cicinelli MV, Capuano V et al. (2016): Optical coherence tomography angiography: a useful tool for diagnosis of treatment-naïve quiescent choroidal neovascularization. *Am J Ophthalmol* **169**: 189–198.
- Chatziralli I, Theodossiadi G, Panagiotidis D, Pousoulidi P & Theodossiadi P (2018): Choriocapillaris vascular density changes in patients with drusen: cross-sectional study based on optical coherence tomography angiography findings. *Ophthalmol Ther* **7**: 101–107.
- Choi W, Mohler KJ, Potsaid B et al. (2013): Choriocapillaris and choroidal microvasculature imaging with ultrahigh speed OCT angiography. *PLoS ONE* **8**: e81499.
- Choi W, Moulton EM, Waheed NK et al. (2015): Ultrahigh-speed, swept-source optical coherence tomography angiography in nonexudative age-related macular degeneration with geographic atrophy. *Ophthalmology* **122**: 2532–2544.
- Cicinelli MV, Rabiolo A, Marchese A, de Vitis L, Carnevali A, Querques L, Bandello F & Querques G (2017): Choroid morphometric analysis in non-neovascular age-related macular degeneration by means of optical coherence tomography angiography. *Br J Ophthalmol* **101**: 1193–1200.
- Cole ED, Moulton EM, Dang S et al. (2017): The definition, rationale, and effects of thresholding in OCT angiography. *Ophthalmol Retina* **1**: 435–447.
- Ding X, Li J, Zeng J, Ma W, Liu R, Li T, Yu S & Tang S (2011): Choroidal thickness in healthy Chinese subjects. *Invest Ophthalmol Vis Sci* **52**: 9555–9560.
- Ferris FL, Wilkinson CP, Bird A, Chakravarthy U, Chew E, Csaky K & Sadda SR (2013): Clinical classification of age-related macular degeneration. *Ophthalmology* **120**: 844–851.
- Fleckenstein M, Charbel Issa P, Helb HM et al. (2008): High-resolution spectral domain-OCT imaging in geographic atrophy associated with age-related macular degeneration. *Invest Ophthalmol Vis Sci* **49**: 4137–4144.
- Flower RW (1993): Extraction of choriocapillaris hemodynamic data from ICG fluorescence angiograms. *Invest Ophthalmol Vis Sci* **34**: 2720–2729.
- Friedman DS, O'Colmain BJ, Munoz B et al. (2004): Prevalence of age-related macular degeneration in the United States. *Arch Ophthalmol* **122**: 564–572.
- Grunwald JE, Hariprasad SM & DuPont J (1998a): Effect of aging on foveolar choroidal circulation. *Arch Ophthalmol* **116**: 150–154.
- Grunwald JE, Hariprasad SM, DuPont J, Maguire MG, Fine SL, Brucker AJ, Maguire AM & Ho AC (1998b): Foveolar choroidal blood flow in age-related macular degeneration. *Invest Ophthalmol Vis Sci* **39**: 385–390.
- Grunwald JE, Metelitsina TI, DuPont JC, Ying GS & Maguire MG (2005): Reduced foveolar choroidal blood flow in eyes with increasing AMD severity. *Invest Ophthalmol Vis Sci* **46**: 1033–1038.
- Howell DC (2010): *Statistical methods for psychology*, 8th edn. Belmont, CA: Cengage Wadsworth. ISBN-13: 978-1-111-83548-4.
- Kvanta A, Casselholm de Salles M, Amrén U & Bartuma H (2017): Optical coherence tomography angiography of the foveal microvasculature in geographic atrophy. *Retina* **37**: 936–942.
- Lane M, Moulton EM, Novais EA et al. (2016): Visualizing the choriocapillaris under drusen: comparing 1050-nm swept-source versus 840-nm spectral-domain optical coherence tomography angiography. *Invest Ophthalmol Vis Sci* **57**: OCT585–OCT590.
- Laueremann JL, Eter N & Alten F (2018): Optical coherence tomography angiography offers new insights into choriocapillaris perfusion. *Ophthalmologica* **239**: 74–84.
- Mancia G, Fagard R, Narkiewicz K, Redon J, Zanchetti A & Bohm M (2013): 2013 ESH/ESC guidelines for the management of arterial hypertension: the Task Force for the Management of Arterial Hypertension of the European Society of Hypertension (ESH) and of the European Society of Cardiology (ESC). *Eur Heart J* **34**: 2159–2219.
- Margolis R & Spaide RF (2009): A pilot study of enhanced depth imaging optical coherence tomography of the choroid in normal eyes. *Am J Ophthalmol* **147**: 811–815.
- McLeod DS, Taomoto M, Otsuji T, Green WR, Sunness JS & Luty GA (2002): Quantifying changes in RPE and choroidal vasculature in eyes with age-related macular degeneration. *Invest Ophthalmol Vis Sci* **43**: 1986–1993.
- McLeod DS, Grebe R, Bhutto I, Merges C, Baba T & Luty GA (2009): Relationship between RPE and choriocapillaris in age-related macular degeneration. *Invest Ophthalmol Vis Sci* **50**: 4982–4991.
- Metelitsina TI, Grunwald JE, DuPont JC, Ying GS, Brucker AJ & Dunaief JL (2008): Foveolar choroidal circulation and choroidal neovascularization in age-related macular degeneration. *Invest Ophthalmol Vis Sci* **49**: 358–363.

- Miller JW, Bagheri S & Vavvas DG (2017): Advances in age-related macular degeneration understanding and therapy. *US Ophthalmic Rev* **10**: 119.
- Mullins RF, Johnson MN, Faidley EA, Skeie JM & Huang J (2011): Choriocapillaris vascular dropout related to density of drusen in human eyes with early age-related macular degeneration. *Invest Ophthalmol Vis Sci* **52**: 1606–1612.
- Nesper PL, Soetikno BT & Fawzi AA (2017): Choriocapillaris non-perfusion is associated with poor visual acuity in eyes with reticular pseudodrusen. *Am J Ophthalmol* **174**: 42–55.
- Nicolò M, Rosa R, Musetti D, Musolino M, Saccheggiani M & Traverso CE (2017): Choroidal vascular flow area in central serous chorioretinopathy using swept-source optical coherence tomography angiography. *Invest Ophthalmol Vis Sci* **58**: 2002–2010.
- de Oliveira Dias JR, Zhang Q, Garcia JM et al. (2018): Natural history of subclinical neovascularization in nonexudative age-related macular degeneration using swept-source OCT angiography. *Ophthalmology* **125**: 255–266.
- Pepple K & Mruthyunjaya P (2011): Retinal pigment epithelial detachments in age-related macular degeneration: classification and therapeutic options. *Semin Ophthalmol* Taylor & Francis, **26**: 124–137.
- Pocock SJ, Assmann SE, Enos LE & Kasten LE (2002): Subgroup analysis, covariate adjustment and baseline comparisons in clinical trial reporting: current practice and problems. *Stat Med* **21**: 2917–2930.
- Querques G, Rosenfeld PJ, Cavallero E, Borrelli E, Corvi F, Querques L, Bandello FM & Zarbin MA (2014): Treatment of dry age-related macular degeneration. *Ophthalmic Res* **52**: 107–115.
- Seddon JM (2017): Macular degeneration epidemiology: nature-nurture, lifestyle factors, genetic risk, and gene-environment interactions – the weisenfeld award lecture. *Invest Ophthalmol Vis Sci* **58**: 6513–6528.
- Spaide RF (2016): Choriocapillaris flow features follow a power law distribution: implications for characterization and mechanisms of disease progression. *Am J Ophthalmol* **170**: 58–67.
- Spaide RF (2017): Choriocapillaris signal voids in maternally inherited diabetes and deafness and in pseudoxanthoma elasticum. *Retina* **37**: 2008–2014.
- Spaide RF, Koizumi H & Pozzoni MC (2008): Enhanced depth imaging spectral-domain optical coherence tomography. *Am J Ophthalmol* **146**: 496–500.
- Spaide RF, Fujimoto JG & Waheed NK (2015): Image artifacts in optical coherence angiography. *Retina* **35**: 2163–2180.
- Spaide RF, Fujimoto JG, Waheed NK, Sadda SR & Staurengi G (2018): Optical coherence tomography angiography. *Prog Retin Eye Res* **64**: 1–55.
- Waheed NK, Moulton EM, Fujimoto JG & Rosenfeld PJ (2016): Optical coherence tomography angiography of dry age-related macular degeneration. *Dev Ophthalmol* **56**: 91–100.
- Wong WL, Su X, Li X, Cheung CMG, Klein R, Cheng CY & Wong TY (2014): Global prevalence of age-related macular degeneration and disease burden projection for 2020 and 2040: a systematic review and meta-analysis. *Lancet Glob Health* **2**: e106–e116.
- Zarbin MA & Rosenfeld PJ (2010): Pathway-based therapies for age-related macular degeneration: an integrated survey of emerging treatment alternatives. *Retina* **30**: 1350–1367.
- Zhang Q, Zheng F, Motulsky EH et al. (2018): A novel strategy for quantifying choriocapillaris flow voids using swept-source OCT angiography. *Invest Ophthalmol Vis Sci* **59**: 203–211.
- Zhu L, Zheng Y, Von Kerczek CH, Topoleski LD & Flower RW (2006): Feasibility of extracting velocity distribution in choriocapillaris in human eyes from ICG dye angiograms. *J Biomech Eng* **128**: 203–209.

Received on June 23rd, 2018.

Accepted on February 21st, 2019.

Correspondence:

Stela Vujosevic, MD, PhD, FEBO
Eye Clinic

University Hospital Maggiore della Carità
Corso Mazzini 18, 28100 Novara
Italy

Tel: +3903213732348

Fax: +3903213732787

Email: stela.vujosevic@gmail.com

This work was completed at the Medical Retina service of the Eye Unit of University Hospital Maggiore della Carità, Novara, Italy.

The authors thank Marco Brambilla, PhD, and Francesco Leporati, Professor, for their help in analysing data.